Electronic Supplementary Material (ESI)

Electronic Supplementary Information

A skeletal randomization strategy for high-performance quinoidal-aromatic polymers

Quanfeng Zhou‡ Cheng Liu‡ Jinlun Li‡ Runze Xie, Guoxiang Zhang, Xiang Ge, Zesheng Zhang, Lianjie Zhang, Junwu Chen, Xiu Gong, Chen Yang, Yuanyu Wang Yi Liu* and Xuncheng Liu**

‡These authors contributed equally

Correspondence —

Xuncheng Liu

College of Materials and Metallurgy

Guizhou University

Guiyang 550025

P. R. China

Email: xcliu3@gzu.edu.cn

1. General methods

Reagents were purchased from Energy Chemical, Innochem, Acros or synthesized as described. Dry solvents were collected from a solvent purification system. Proton and carbon nuclear magnetic resonance spectra (^{1}H-NMR and ^{13}C-NMR) spectra were recorded on a JNM-ECZ400S/L1 spectrometer. All chemical shifts are quoted using the δ scale, and all coupling constants (J) are expressed in Hertz (Hz). Cyclic voltammetry (CV) was carried out on a CHI600E electrochemical workstation with platinum electrodes at a scan rate of 50 mV s^{-1} against an Ag/Ag$^+$ reference electrode with nitrogen-saturated solution of 0.1 M tetrabutylammonium hexafluorophosphate (Bu_4NPF_6) in acetonitrile (CH_3CN). Potentials were referenced to the ferrocenium/ferrocene couple by using ferrocene as an internal standard. The molecular weight of polymer was determined by high temperature size exclusion chromatography (SEC) at 140 °C using a calibration curve of polystyrene standards, with 1,2,4-trichlorobenezene as the eluent. Thermogravimetric (TGA) measurements were carried out with a NETZSCH (TG550) apparatus at a heating rate of 20 °C /min under a nitrogen atmosphere. Differential scanning calorimetry (DSC) analysis were taken on TAQ 2000 under a nitrogen atmosphere at a rate of 10 °C/min from 25 to 250 °C, and then cooling to 25 °C. The FTIR measurements were carried out with a Bruker VERTEX 70 spectrometer equipped with an ATR attachment. UV-Vis-NIR spectra were recorded using a MAPADA UV-6300 spectrometer. GIWAXS measurements were accomplished with a Xeuss 2.0 SAXS/WAXS laboratory beamline using a Cu X-ray source (8.05 keV, 1.54 Å) and a Pilatus3R 300K detector. The incidence angle is 0.2°. Scattering pattern was collected with a Dectris Pilatus3R 1M area detector. Atomic force microscopy (AFM) images were obtained with a Bruker Dimension ICON, using tapping mode in air under ambient conditions.

2. Synthesis procedures

(Z)-1-acetyl-3-((5-bromothiophen-2-yl)methylene)piperazine-2,5-dione (2)

A mixture of **1** (396.4 mg, 2 mmol, 1 eq.), 5-Bromothiophene-2-carbaldehyde (401.2 mg, 2.1 mmol, 1.05 eq), Cs_2CO_3 (684.2 mg, 2.1 mmol, 1.05 eq.) was dissolved in 40 mL of anhydrous DMF under N_2 protection. The reaction mixture was stirred at room temperature for 8h. Then crushed ice was added to stand for one hour and yellow precipitate was formed, the precipitate was collected by filtration and rinsed with ethyl alcohol. Yield: 74%. ^{1}H NMR ($CDCl_3$, 400 MHz, 298 K) δ = 7.74 (s, 1H), 7.19 (s, 1H), 7.13 (d, J = 4.0 Hz, 1H), 7.07 (d, J = 3.9 Hz, 1H), 4.53 (s, 2H), 2.63 (s, 3H). ^{13}C NMR ($CDCl_3$, 101 MHz, 298 K) δ = 172.42, 162.83, 160.15, 136.99, 131.45, 131.12, 123.87, 116.73, 112.63, 46.07, 27.24.

(3Z,6Z)-3-((5'-bromo-[2,2'-bithiophen]-5-yl)methylene)-6-((5-bromothiophen-2-yl)methylene)piperazine-2,5-dione (3)

Into a mixture of **2** (1975.0 mg 6.0 mmol, 1 eq.) and 5'-bromo-[2,2'-bithiophene]-5-carbaldehyde (1966.8 mg, 7.2 mmol, 1.2 eq.) in DMF (30 mL) was syringe injected triethylamine (25 mmol, 4 eq.) at 120 °C under N_2 protection. Upon addition, the original colorless solution turned red immediately. Orange precipitate was formed during the overnight reaction. After cooling to room temperature, the precipitate was collected by filtration and rinsed with acetone. The product was used for next steps without further purification. Yield: 85%.

Monomer (4)

A mixture of the compound **3** (542.28 mg, 1mmol, 1 eq.), K_2CO_3 (552.8 mg, 4 mmol, 4 eq.) and 11-(bromomethyl)tricosane (1461.4 mg, 3.5 mmol, 3.5 eq.) in DMF (30 mL) was stirred at 100 °C for 4 hours under N_2 protection. After cooling to room temperature, the reaction mixture was filtered, and the filtrate was concentrated by rotary evaporation under reduced pressure. And the crude product was purified by silica gel chromatography (Hexane: $CHCl_3$ (9:1 [v/v]) to afford the desired product red solid. Yield: 51%. ^{1}H NMR ($CDCl_3$, 400 MHz, 298 K) δ = 7.17 (d, J = 3.8 Hz, 1H), 7.08 (d, J = 3.7 Hz, 2H), 7.02 (dd, J = 9.0, 4.0 Hz, 3H), 6.96 (d, J = 3.7 Hz, 1H), 6.93 (d, J = 3.9 Hz, 1H), 4.41 (dd, J = 13.7, 6.0 Hz, 4H), 1.95 (s, 2H), 1.41-1.20 (m, 80H), 0.87 (t, J = 5.8 Hz, 12H). ^{13}C NMR ($CDCl_3$, 101 MHz, 298 K) δ = 158.03, 157.80, 140.88, 140.82, 139.78, 138.65, 131.44, 130.85, 129.89, 129.26, 128.72, 128.55, 123.32, 118.69, 116.78, 116.35, 111.36, 71.34, 37.39, 37.28, 32.05, 31.75, 30.27, 30.24, 29.85, 29.80, 29.50, 26.93, 22.82, 14.26.

Polymer PA4T-L

A mixture of monomer **5** (283.36 mg, 0.25 mmol, 1 eq.), 5,5'-bis(trimethylstannyl)-2,2'-bithiophene (122.96 mg, 0.25 mmol, 1 eq.), $Pd(PPh_3)_4$ (8.65 mg, 7.5 µmol, 0.03 eq.) in toluene (10 mL) was sealed in a Ar flushed vessel and heated to 80 °C while stirring for 6 h. 2-Trimethyltin thiophene (0.2 mL) and bromobenzene (0.2 mL) were injected successively as end-capping reagents. The reaction mixture was stirred for 2 h after each injection.After cooling down, the mixture was precipitated into methanol. The precipitate collected from filtration was subjected to Soxhlet extraction with methanol, acetone, ethyl acetate, CF and CB successively.

The CB fraction was concentrated and precipitated into methanol. The polymer PA4T-L was collected by filtration.

Polymer PA4T-C12-1

A mixture of monomer **5** (283.36 mg, 0.25 mmol, 1 eq.), (3,3'-didodecyl-[2,2'-bithiophene]-5,5'-diyl)bis(trimethylstannane) (207.13 mg, 0.25 mmol, 1 eq.), $Pd(PPh_3)_4$ (8.65 mg, 7.5 µmol, 0.03 eq.) in toluene (10 mL) was sealed in a Ar flushed vessel and heated to 100 °C while stirring for 24 h. 2-Trimethyltin thiophene (0.2 mL) and bromobenzene (0.2 mL) were injected successively as end-capping reagents. The reaction mixture was stirred for 2 h after each injection.After cooling down, the mixture was precipitated into methanol. The precipitate collected from filtration was subjected to Soxhlet extraction with methanol, acetone, ethyl acetate and CF successively. The CF fraction was concentrated and precipitated into methanol. The polymer PA4T-C12-1 was collected by filtration.

Polymer PA4T-C12-2

A mixture of monomer **5** (283.36 mg, 0.25 mmol, 1 eq.), (4,4'-didodecyl-[2,2'-bithiophene]-5,5'-diyl)bis(trimethylstannane) (207.13 mg, 0.25 mmol, 1 eq.), $Pd(PPh_3)_4$ (8.65 mg, 7.5 µmol, 0.03 eq.) in toluene (10 mL) was sealed in a Ar flushed vessel and heated to 100 °C while stirring for 24 h. 2-Trimethyltin thiophene (0.2 mL) and bromobenzene (0.2 mL) were injected successively as end-capping reagents. The reaction mixture was stirred for 2 h after each injection.After cooling down, the mixture was precipitated into methanol. The precipitate collected from filtration was subjected to Soxhlet extraction with methanol, acetone, ethyl acetate and CF successively. The CF fraction was concentrated and precipitated into methanol. The polymer PA4T-C12-2 was collected by filtration.

Polymer PA4T-Ra

A mixture of monomer **4** (303.89 mg, 0.25 mmol, 1 eq.), 2,5-bis(trimethylstannyl) thiophene (102.43 mg, 0.25 mmol, 1 eq.), $Pd(PPh_3)_4$ (8.65 mg, 7.5 µmol, 0.03 eq.) in toluene (10 mL) was sealed in a Ar flushed vessel and heated to 100 °C while stirring for 24 h. 2-Trimethyltin thiophene (0.2 mL) and bromobenzene (0.2 mL) were injected successively as end-capping reagents. The reaction mixture was stirred for 2 h after each injection.After cooling down, the mixture was precipitated into methanol. The precipitate collected from filtration was subjected to Soxhlet extraction with methanol, acetone, ethyl acetate, $CHCl_3$ (CF) and chlorobenzene (CB) successively. The CB fraction was concentrated and precipitated into methanol. The polymer PA4T-Ra was collected by filtration.

3. Fabrication and characterization of organic field-effect transistors (OFETs)

Organic field-effect transistors were fabricated in a typical bottom gate, top contact architecture. Transistors were fabricated with highly doped Si as the gated electrode, gold (Au) as both source and drain electrodes. Substrates were cleaned by successive sonication with soap water, deionized water, acetone and absolute ethanol. Then the substrate gate dielectric layers were modified by *n*-octadecyltrichlorosilane (OTS) by submersion in a solution of OTS in toluene. The polymer solutions were prepared in 5 mg mL^{-1} CB/CF (mixture solvent, volume ratio = 1:6) and stirred on a hot plate overnight. Before spin coating, polymer solutions were cooled to room temperature naturally. Then, polymer solutions were spin-coated (2500 rpm, 30 s) onto the substrates at room temperature to form polymer thin films in ambient air. When thermal treatment was noted, the polymer films were annealed at 200 °C for 10 minutes on a hotplate in a nitrogen glovebox. Gold contacts (40 nm) were evaporated on the polymer film layer through a metal mask to define channels of 80 μm in length and 1400 μm in width. The film thickness of the devices ranges from 60 to 100 nm. Field effect mobility was calculated from the standard equation for saturation region in metal-dioxide-semiconductor field effect transistors: $I_{ds} = \mu\ (W/2L)\ C_i\ (V_g - V_t)^2$, where I_{ds} is drain-source current, μ is field effect mobility, W and L are the channel width and length, C_i is the capacitance per unit area of the gate insulator (C_i = 10 nF/cm^2), V_g is the gate voltage and V_t is the threshold voltage.

4. Theoretical calculations

For simplicity, the alkyl chains were all replaced by methyl groups. Density functional theory (DFT) calculations of a tetramer segments of polymers were performed using Gaussian 09[1] at the B3LYP[2]/6-311g (d, p)[3, 4] level with the D3 (BJ) empirical dispersion correction[5]. The calculation of band structures and density of states of the polymers were performed using Vienna ab initio simulation package (VASP)[6] with the Perdew-Burke-Ernzerhof (PBE) functional instead of B3LYP functional due to its mild demands of computational resources and the importance of being consistent with previous related studies.[7] Uniform 21 × 1 × 1 Monkhorst-Pack *k*-point mesh was used for structural optimization. The energy cut off for the plane-wave expansion was set to 400 eV and the force criteria was less than 0.05 eV/Å. 41 *k*-points were calculated between the gamma point and the edge of the first BZ to afford band structure and density of states. The hole effective mass (m_h*)[8] for 1D crystal is calculated based on band structure by the equation:

$m_h^* = h^2 / (d^2E/dk^2)$

Where E is the band energy and *k* is the electron wave vector along backbone direction.

5. Solubility Limit Measurement

Solubilities of five polymers were measured by a standard calibration curve method.[9, 10] First, to construct standard calibration curves, the absorbance of different concentrations of five polymers (0.01−0.05 mg/mL) CB solutions were measured. Next, the polymer powder was gradually added to the solution until saturation was achieved, the CB solution was stirred at 80°C for two hours. Subsequently, the solution was cooled to room temperature and centrifuged (e.g., 10000 rpm for 30 min). Lastly, the top clear solution in each centrifuge tube was selected, and the solubility of each material was determined by measuring its absorbance after dilution with a saturated solution and using individual standard curves.

6. Additional Figures

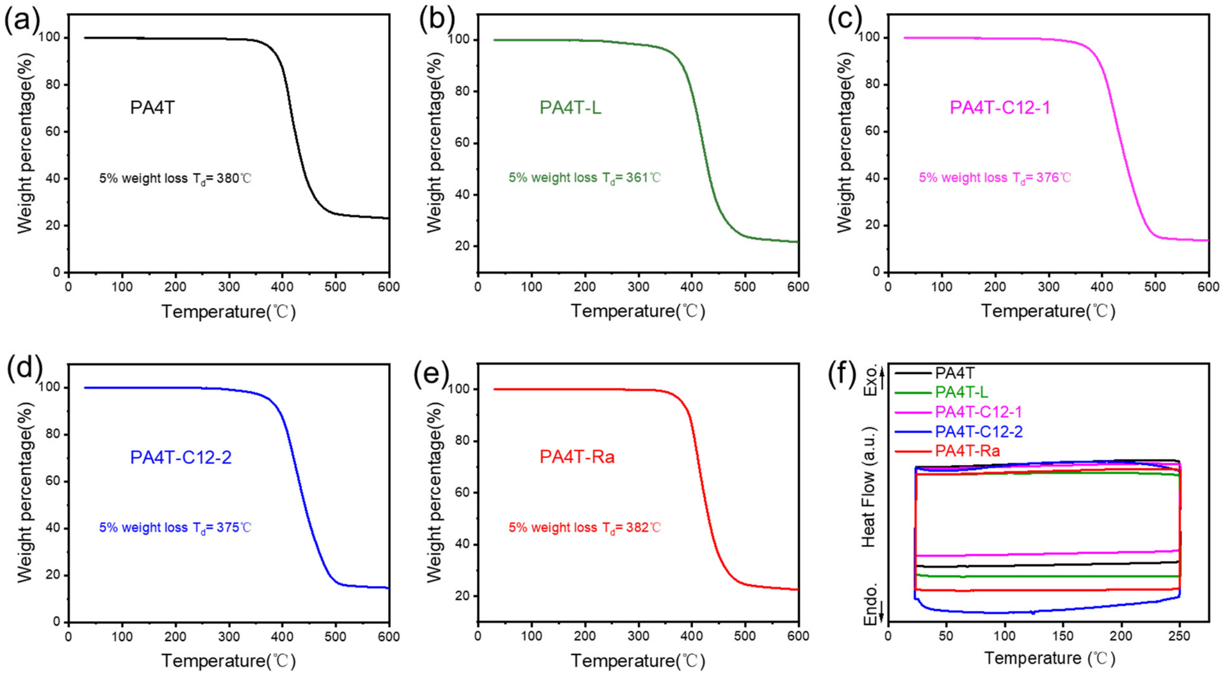

Figure S1. Thermogravimetric analysis (TGA) and differential scanning calorimetry (DSC) analysis curves of five polymers.

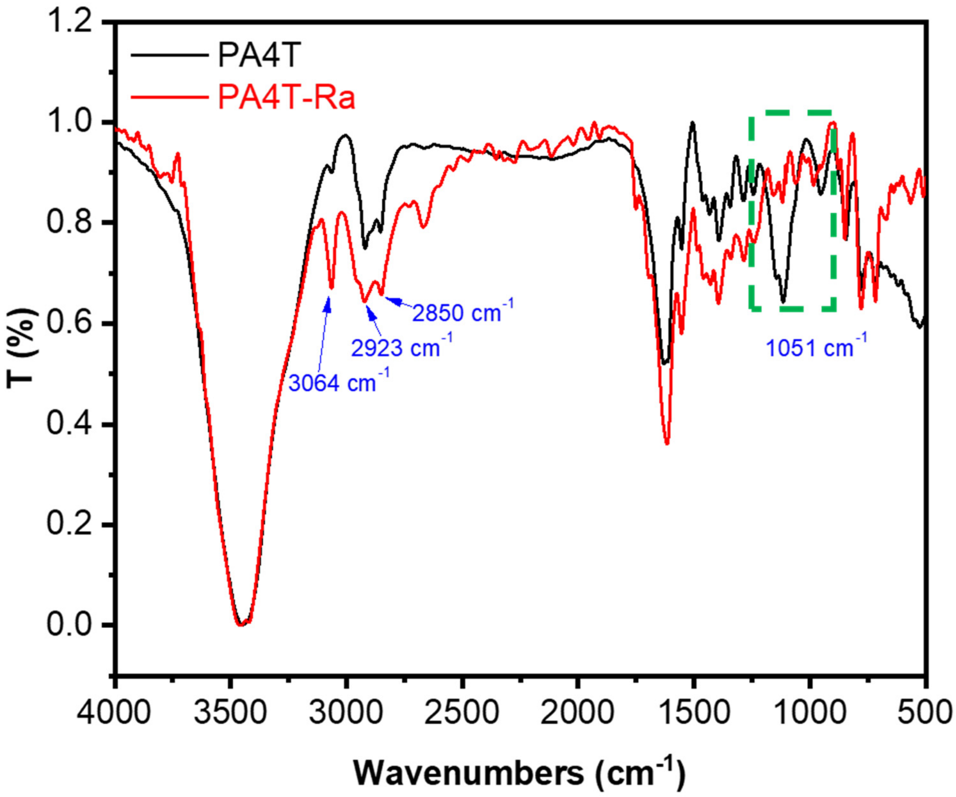

Figure S2. FTIR spectra of PA4T, PA4T-Ra.

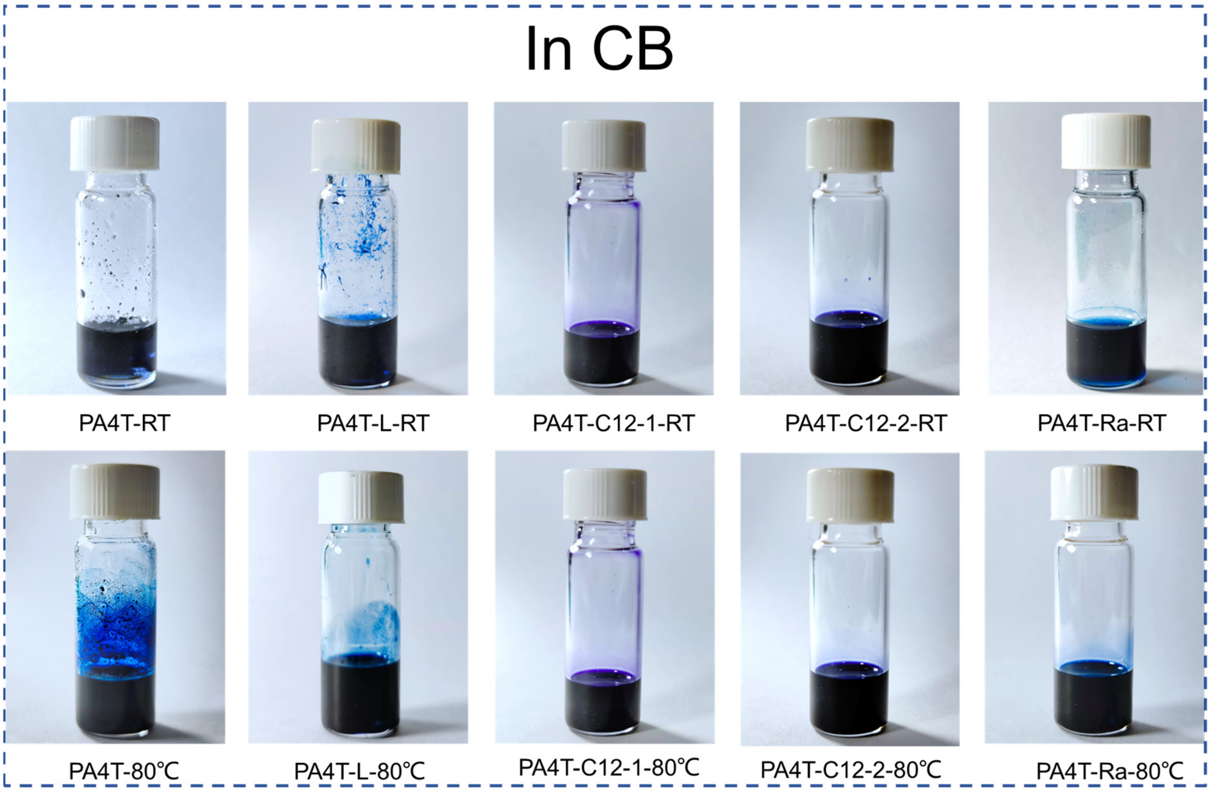

Figure S3. Photographs of five polymers in CB.

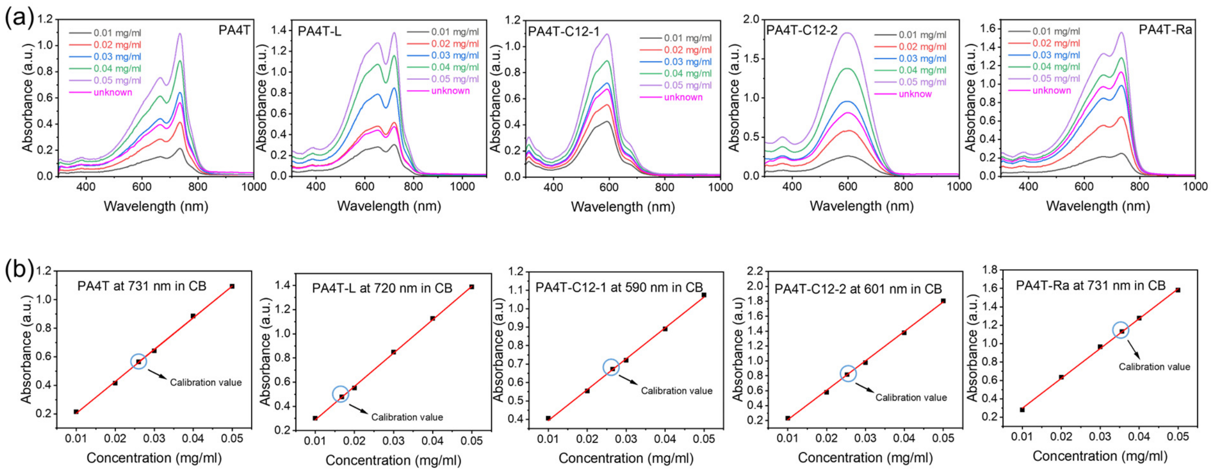

Figure S4. Absorption spectra for determining the solubility of five polymers in 80 °C chlorobenzene: a) absorption spectra of standard solutions of five polymers, respectively. b) plot of absorbance at a certain wavelength (as indicated in the figures) versus concentration. The unknown PA4T, PA4T-L, PA4T-C12-1,PA4T-C12-2 and PA4T-Ra based samples were prepared by dilution of 200, 500, 2000, 2000 and 500 times from saturated solution.

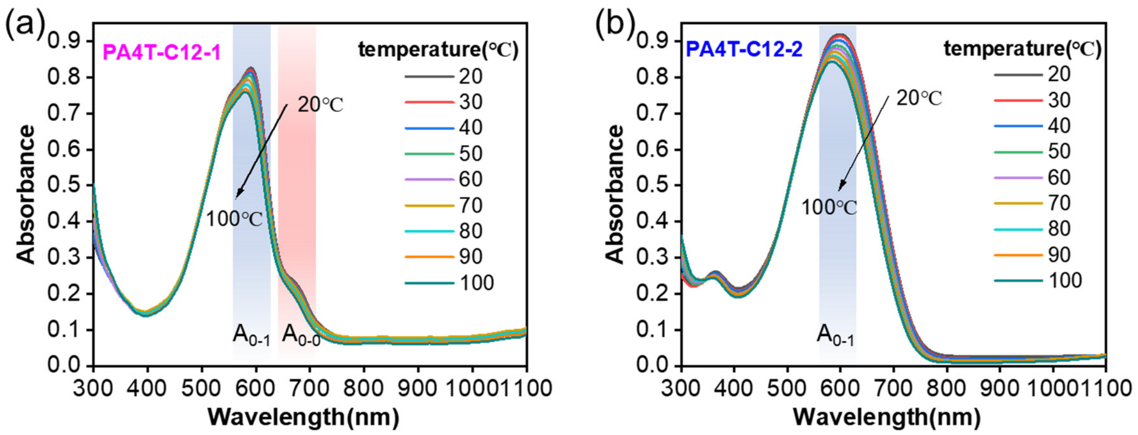

Figure S5. The evolution of UV-vis absorption spectra of a) PA4T-C12-1 and b) PA4T-C12-2 in chlorobenzene during a heating process.

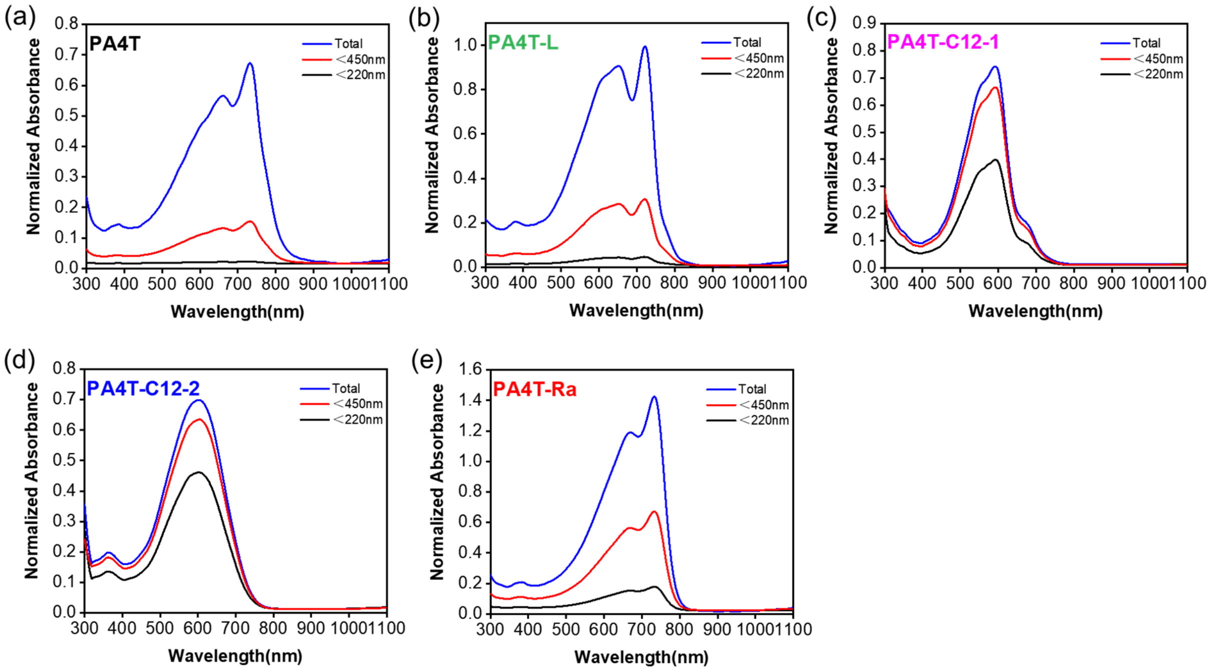

Figure S6. Absorption spectra of five polymer solution in the filtration experiments[11].

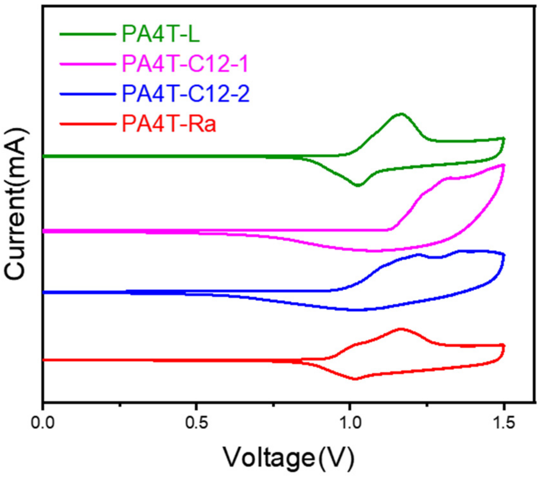

Figure S7. Cyclic voltammetry curves of polymers at a scan rate of 100 mV/s.

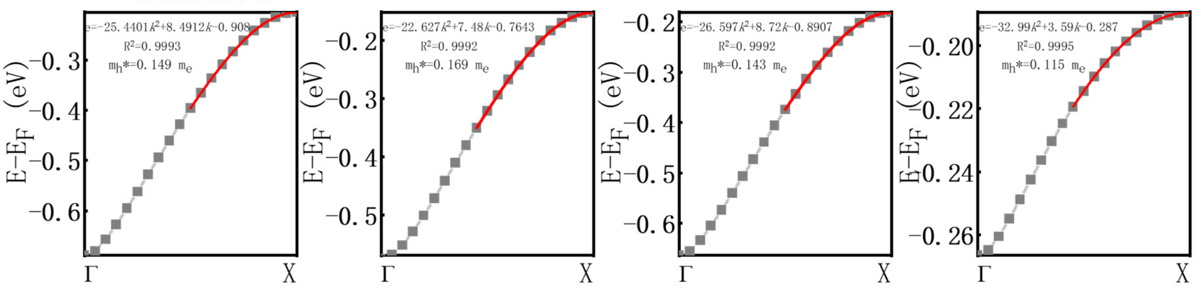

Figure S8. Curve fitting based on band structure to obtain the hole effective mass for polymers.

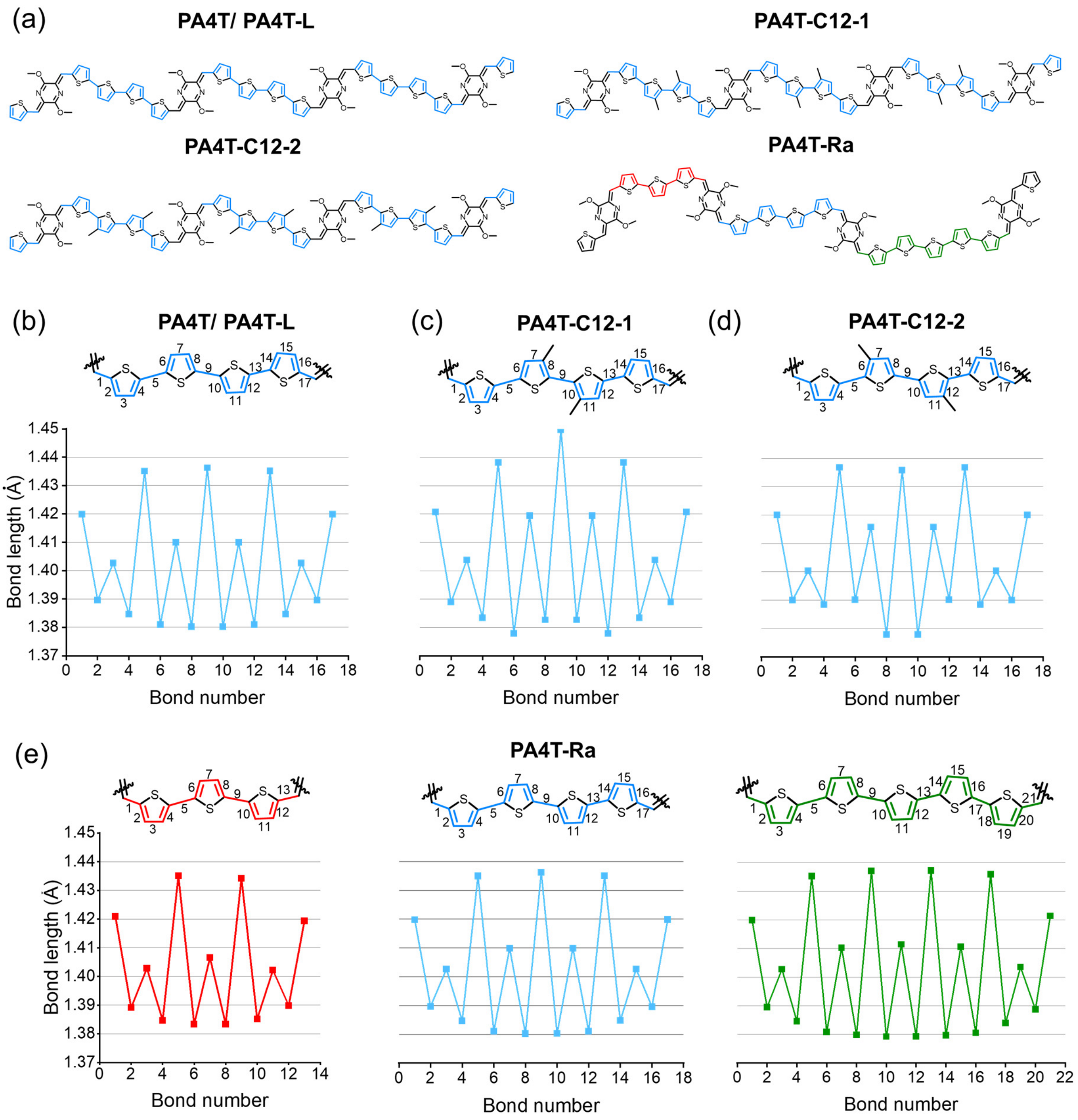

Figure S9. a) Chemical structure of the tetramer of five polymers. Plots of carbon−carbon bond length for each respective bond number in the quaterthiophene unit in b) PA4T/PA4T-L, c) PA4T-C12-1 and d) PA4T-C12-2, which were extracted from the central quaterthiophene unit of the tetramer models. Plot of carbon−carbon bond length for each respective bond number in three oligothiophene segments in e) PA4T-Ra.

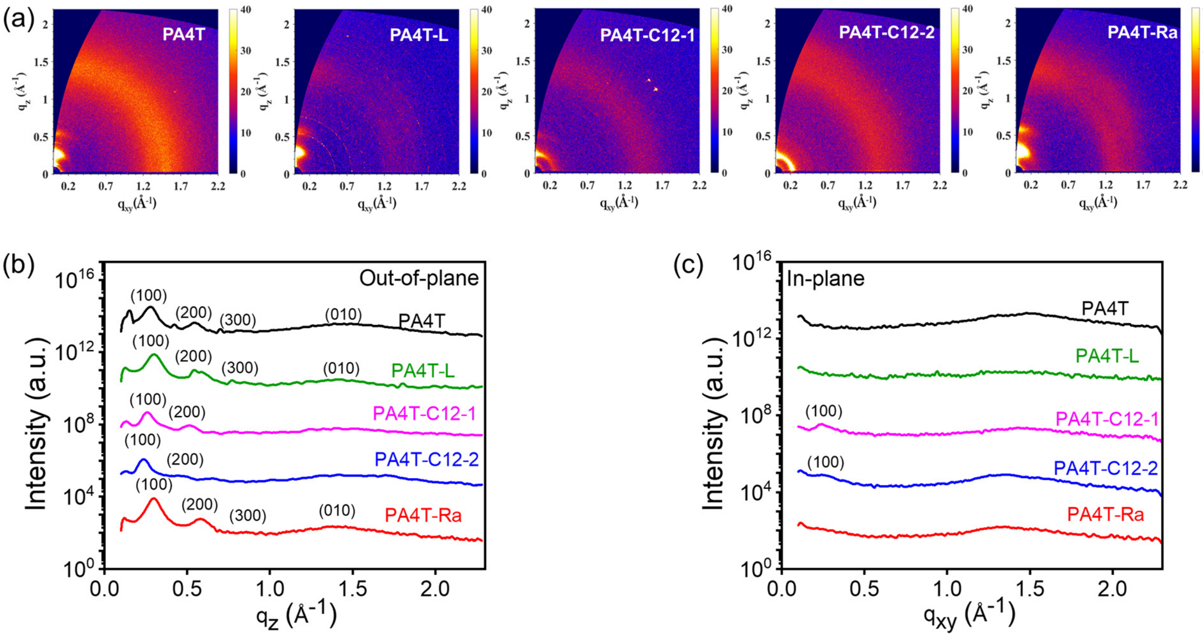

Figure S10. a) GIWAXS patterns. Line-cut profiles along b) out-of-plane and c) in-plane directions of as-cast polymer films.

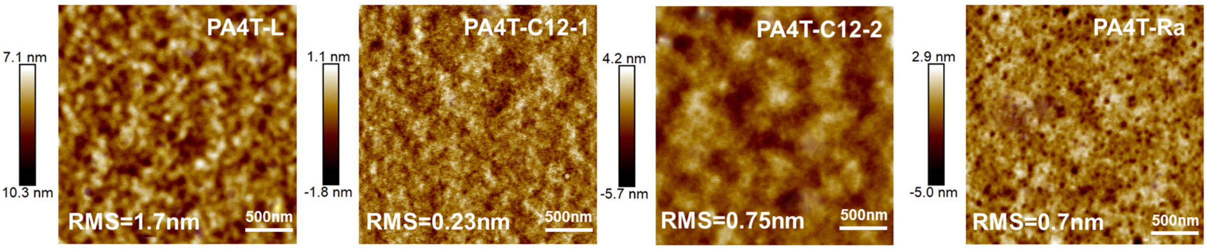

Figure S11. AFM images of as-cast polymer films.

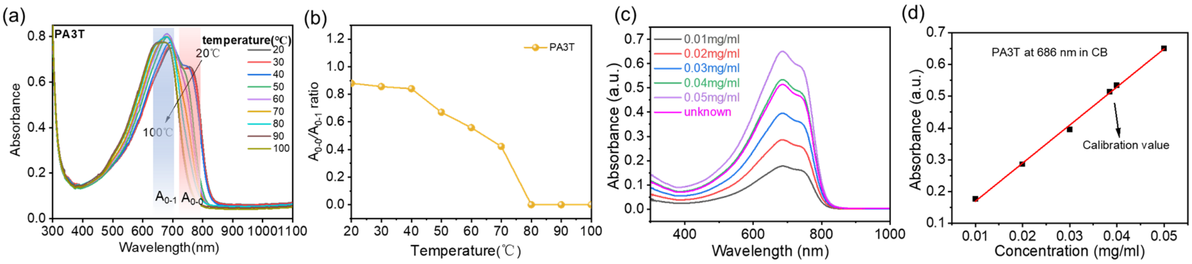

Figure S12. a) The evolution of UV-vis absorption spectra of PA3T in chlorobenzene during heating process. b) A_{0-0}/A_{0-1} ratio of PA3T extracted from varied temperature UV-vis absorption spectra. Absorption spectra for determining the solubility of PA3T in 80 °C chlorobenzene: c) absorption spectra of standard solutions of PA3T. d) plot of absorbance at a certain wavelength (as indicated in the figures) versus concentration. The unknown PA3T based samples were prepared by dilution of 200, 500, 2000, 2000 and 500 times from saturated solution.

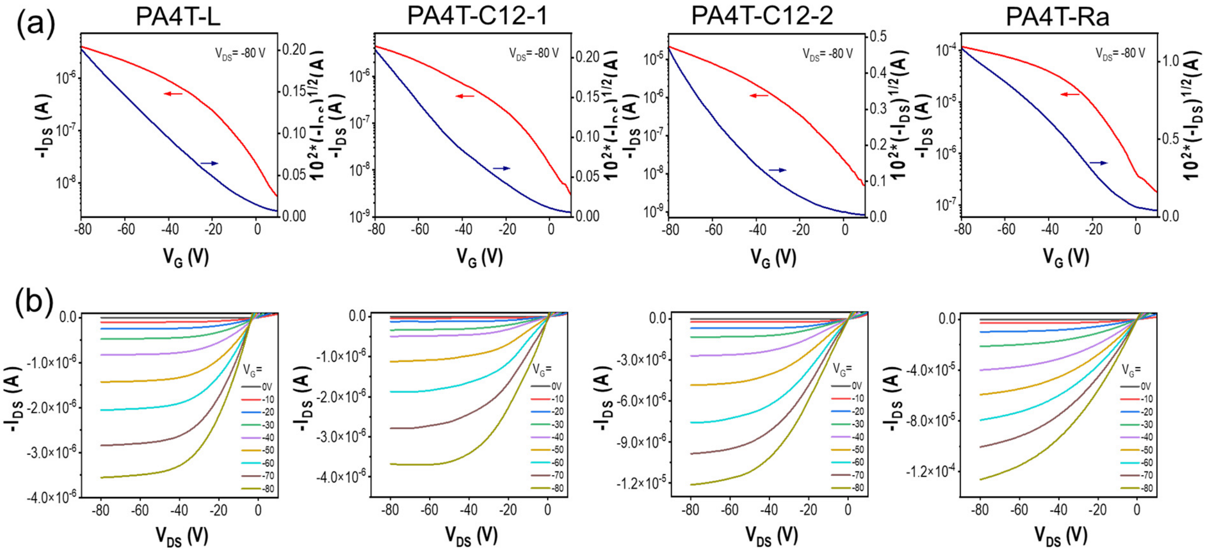

Figure S13. Typical a) transfer and b) output characteristics of OFETs without thermal annealing.

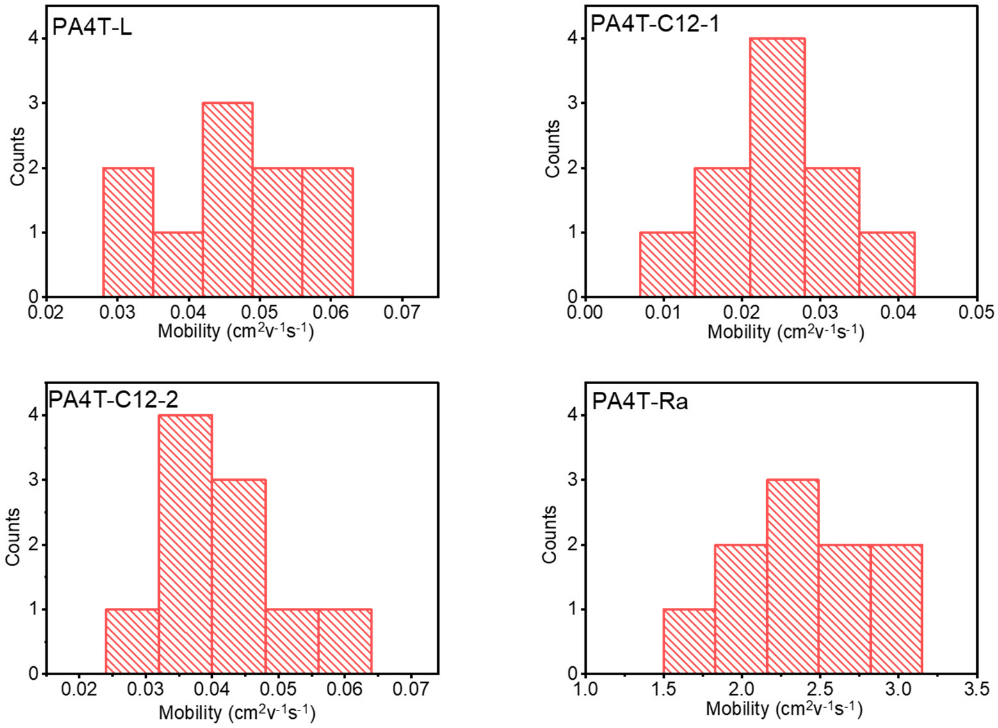

Figure S14. The mobility statistic graph of annealed films.

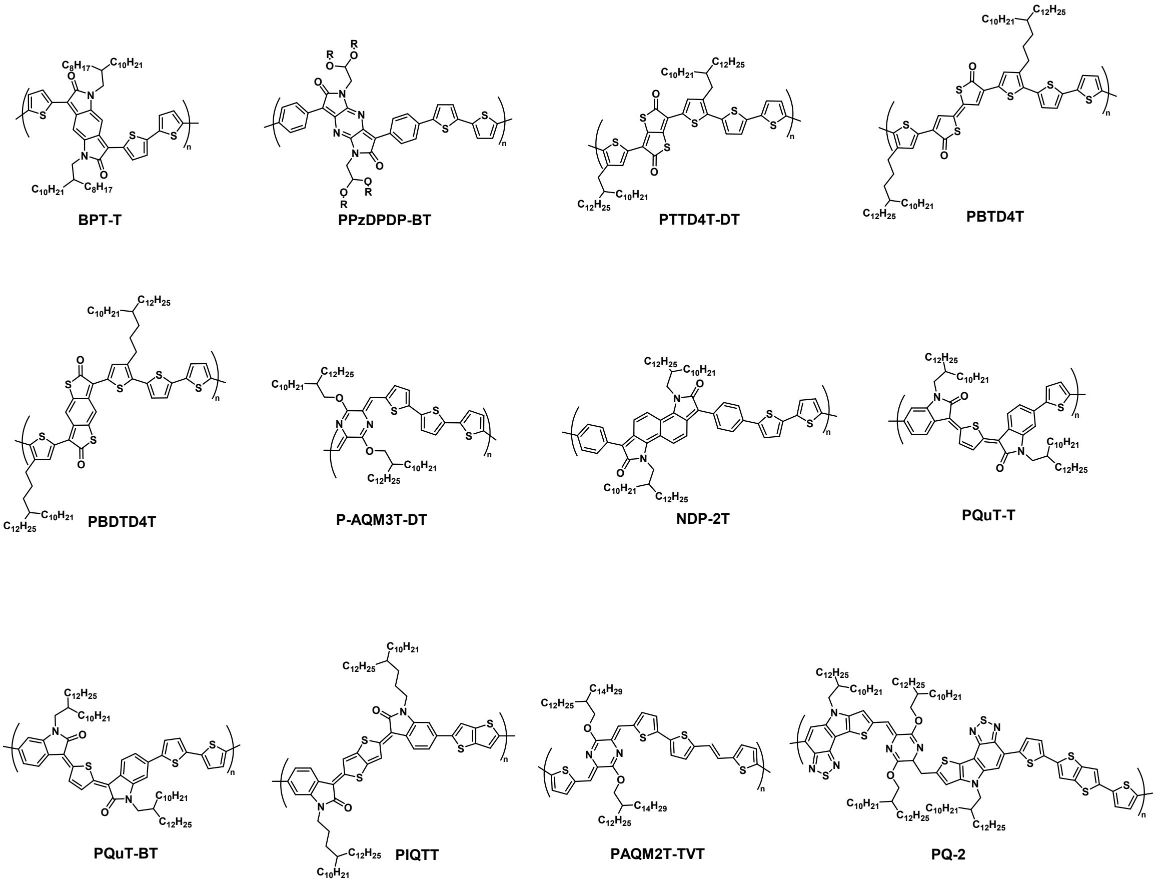

Figure S15. Chemical structures from the literature of quinoid-donor polymers based on ground-state quinoidal units in recent 10 years.

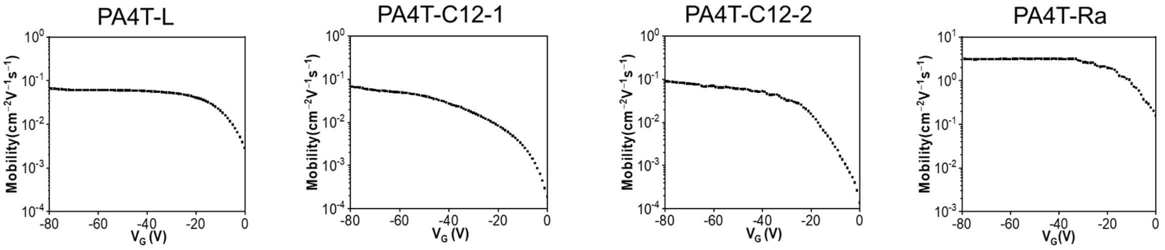

Figure S16. Mobility *versus* gate voltage plot of the OFETs based on PA4T-L, PA4T-C12-1, PA4T-C12-2 and PA4T-Ra.

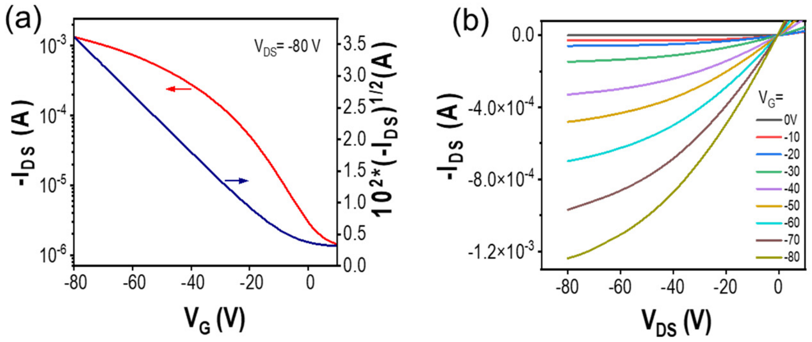

Figure S17. Typical a) transfer and b) output characteristics of annealed OFETs based on the second batch of polymer PA4T-Ra.

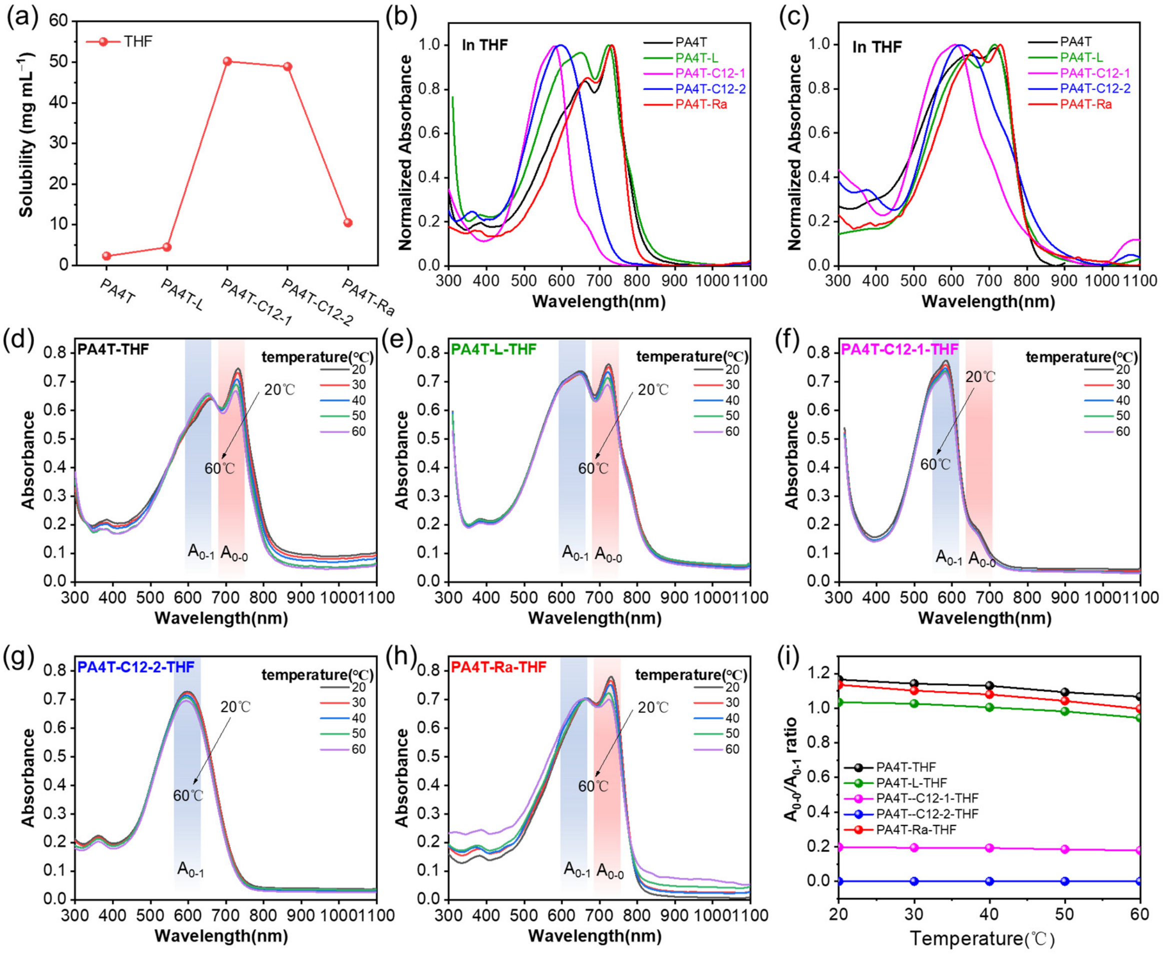

Figure S18. Solubilities of the five polymers in THF at 60 °C. Normalized UV-vis absorption spectra of the five polymers b) in chlorobenzene and c) thin film at room temperature. d-h) The evolution of UV-vis absorption spectra of the five polymers in THF upon heating. i) A_{0-0}/A_{0-1} ratios of the five polymers extracted from variable temperature UV-vis absorption spectra.

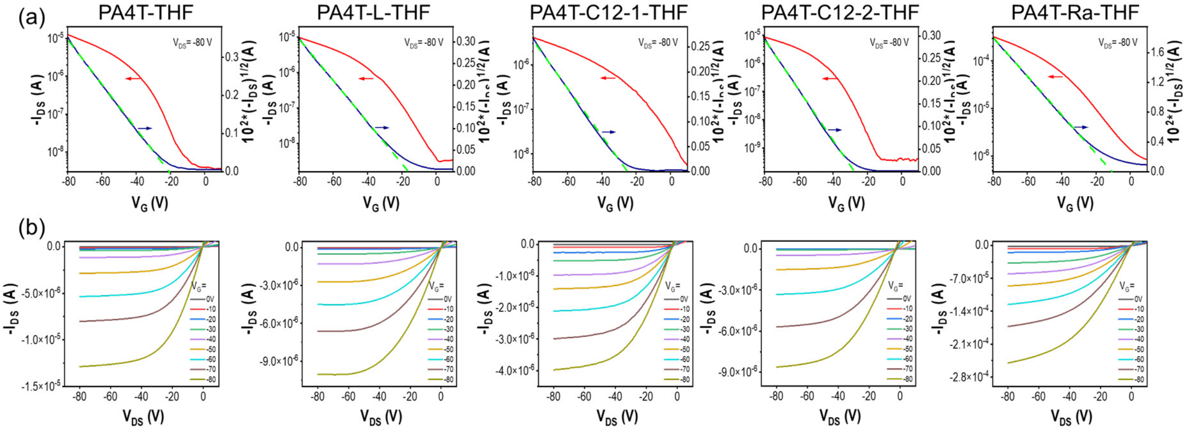

Figure S19. Typical a) transfer and b) output characteristics of annealed OFETs based on the five polymers using THF.

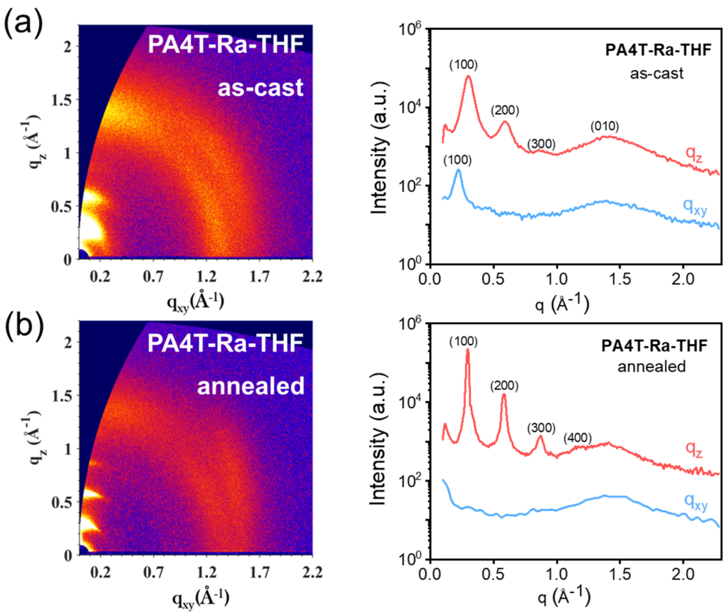

Figure S20. GIWAXS patterns and line-cut profiles along out-of-plane and in-plane directions of a) as cast and b) annealed PA4T-Ra film processed from THF.

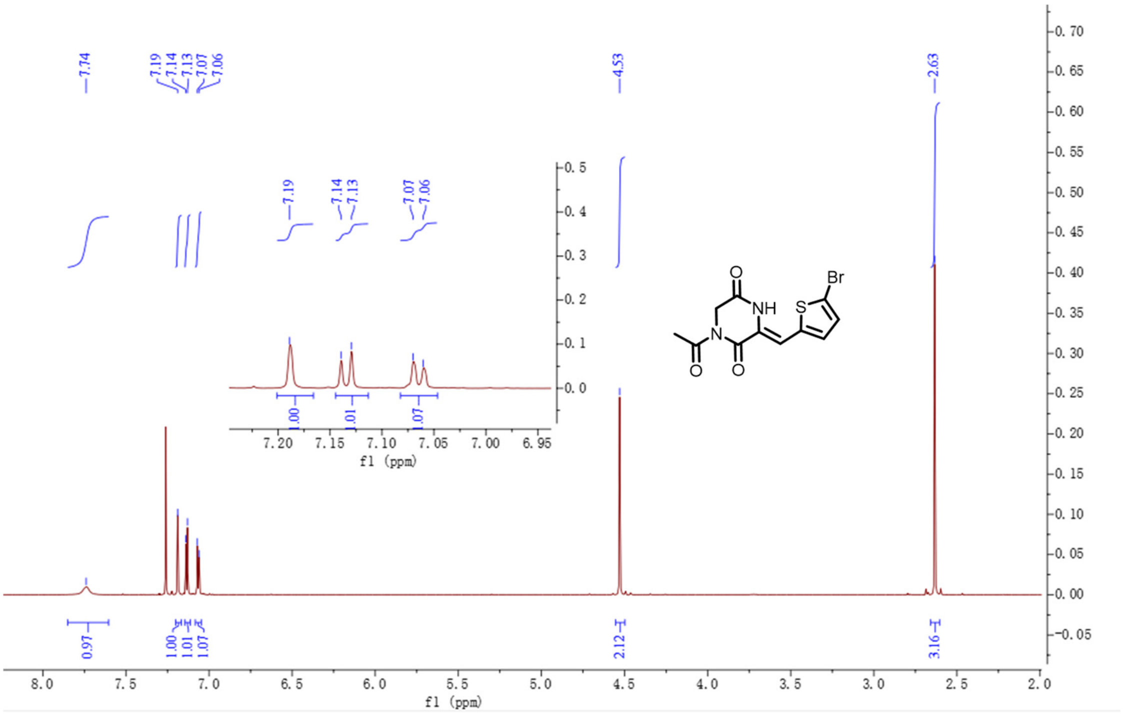

Figure S21. ^{1}H NMR spectrum of compound 2 ($CDCl_3$, 298 K).

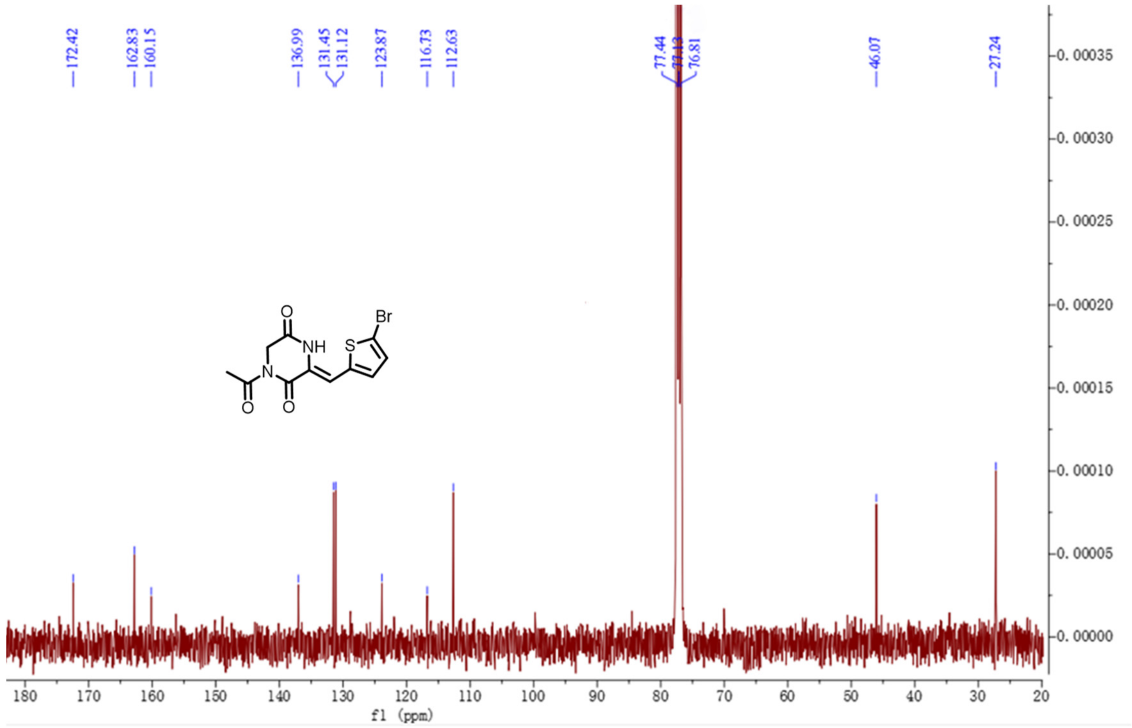

Figure S22. ^{13}C NMR spectrum of compound 2 ($CDCl_3$, 298 K).

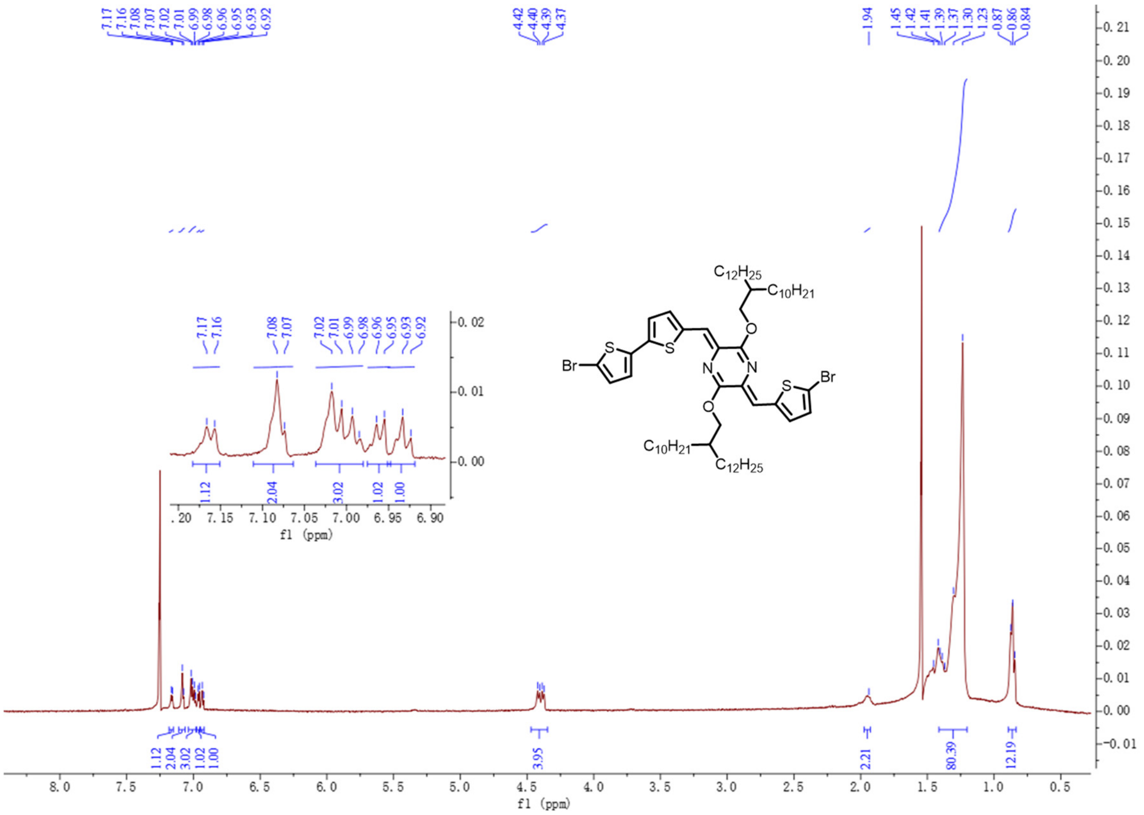

Figure S23. ^{1}H NMR spectrum of monomer 4 ($CDCl_3$, 298 K).

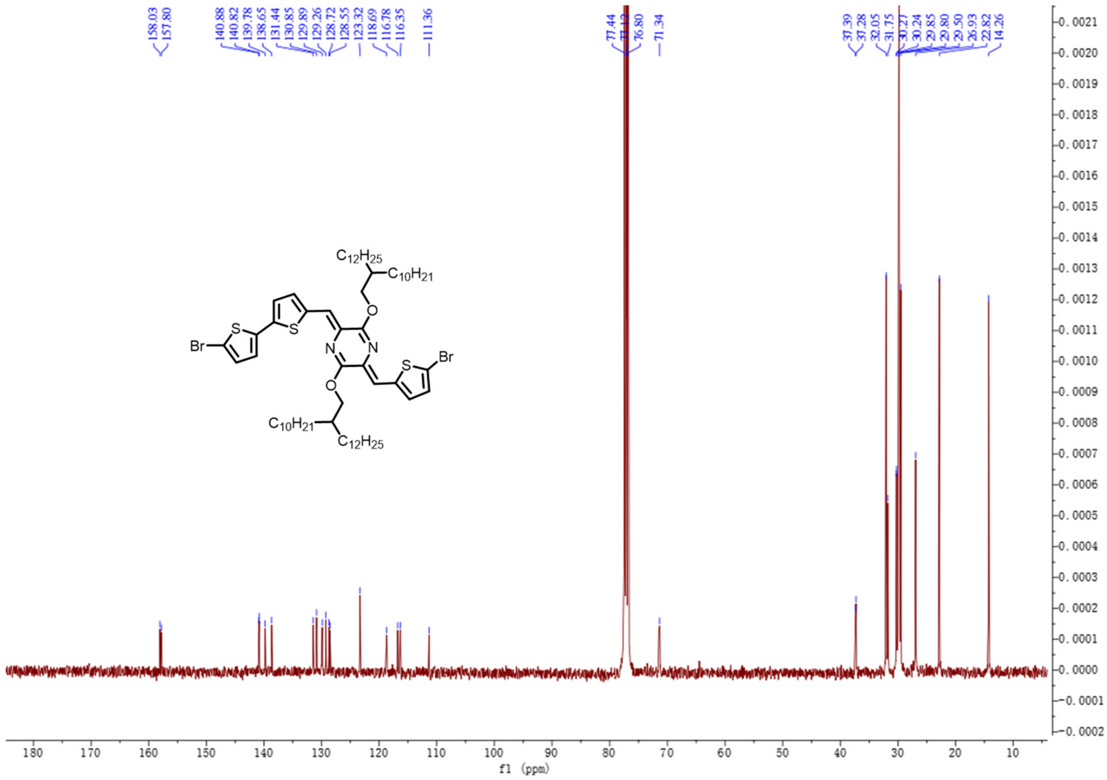

Figure S24. ^{13}C NMR spectrum of monomer 4 ($CDCl_3$, 298 K).

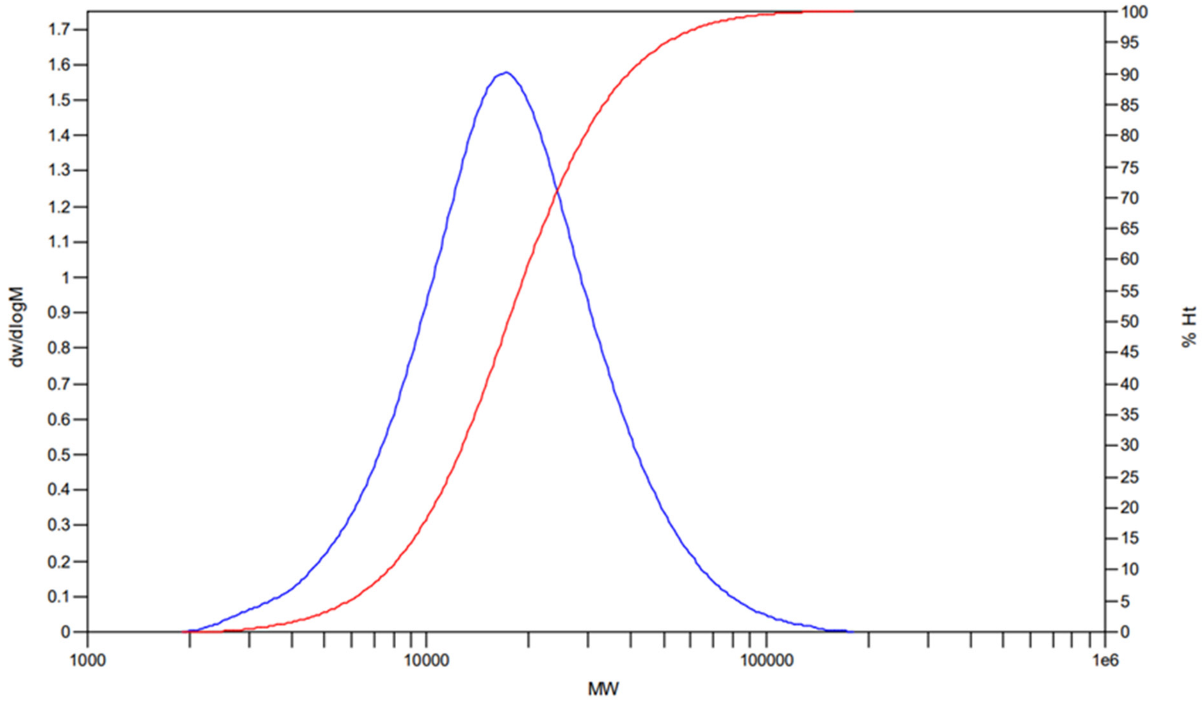

Figure S25. SEC distribution plots of PA4T-L with 1,2,4-trichlorobenezene as the eluent at 140 °C.

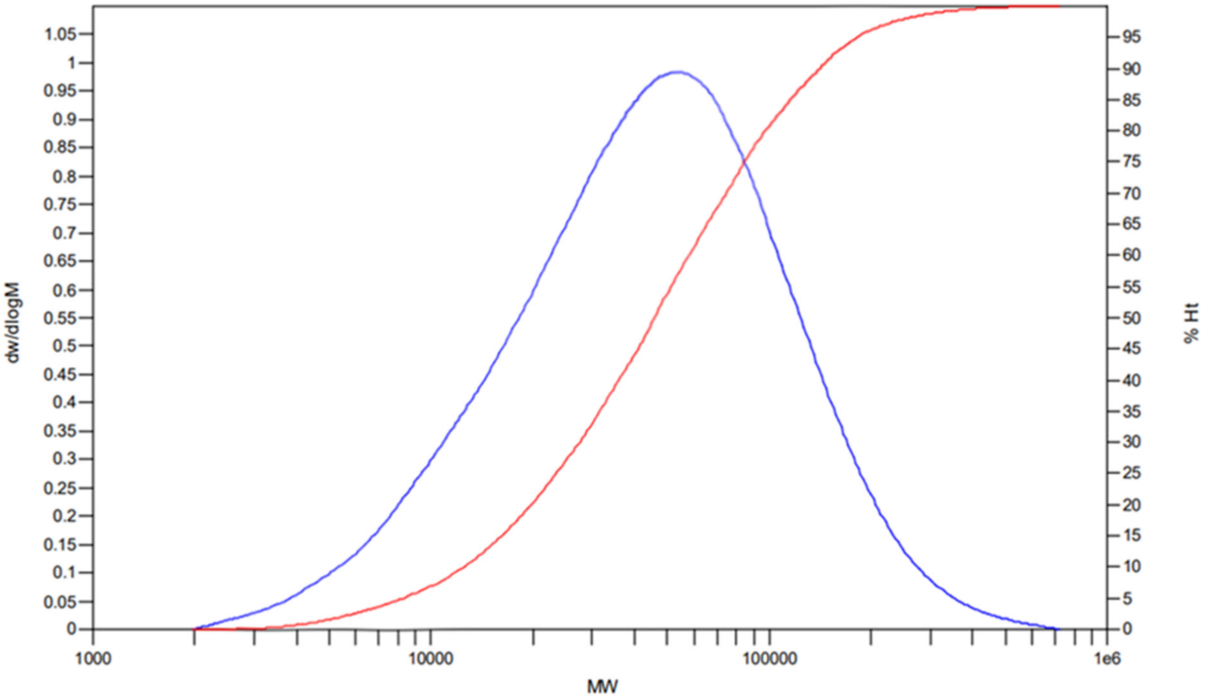

Figure S26. SEC distribution plots of PA4T-C12-1 with 1,2,4-trichlorobenezene as the eluent at 140 °C.

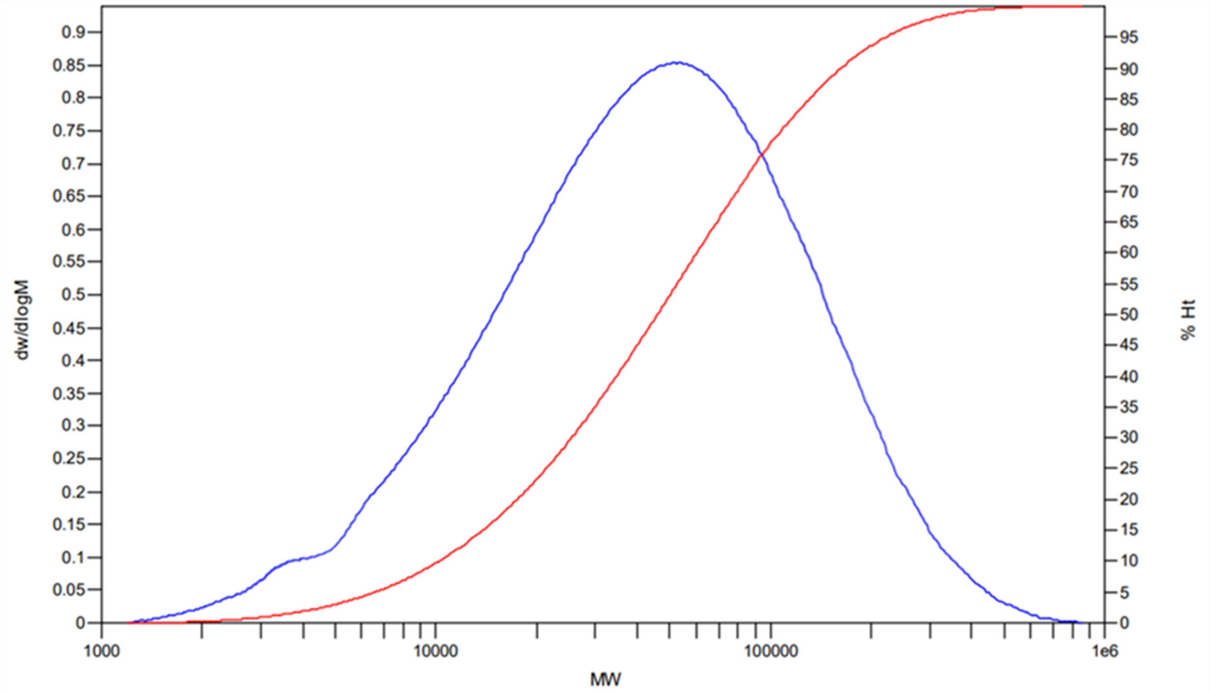

Figure S27. SEC distribution plots of PA4T-C12-2 with 1,2,4-trichlorobenezene as the eluent at 140 °C.

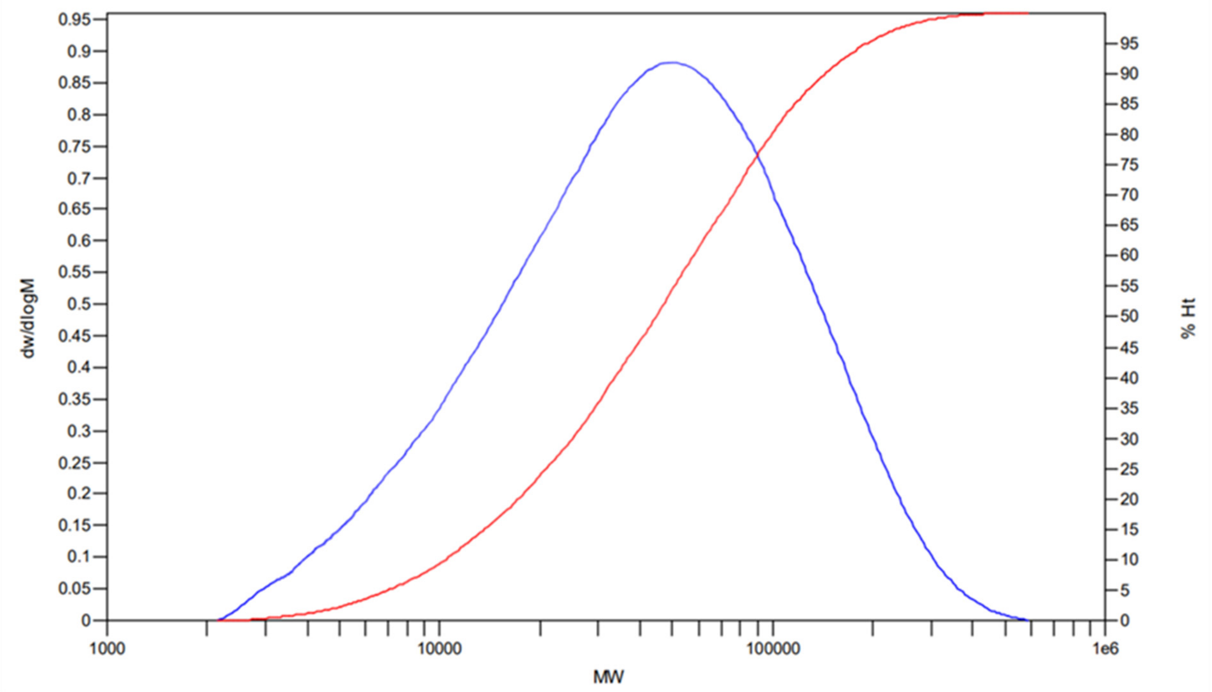

Figure S28. SEC distribution plots of PA4T-Ra with 1,2,4-trichlorobenezene as the eluent at 140 °C.

7. Complementary data

Table S1. Solubility of PA3T and GIWAXS data of annealed PA3T.

Polymer	Solubility[a] [mg mL^{-1}]	Lamellar d-spacing[b] (Å)	CCL[c] (Å)	*g* factor[c] (%)
PA3T	23.1	22.3	205	12.8

[a]In chlorobenzene at 80 °C. [b]Reported previously. [c] Crystalline coherence length and *g* factor were calculated according to OOP (200) diffraction peaks.

Table S2. OFET performances of the polymers processed from chlorinated solvent.

Polymer	$T_{annealing}$ [°C]	$\mu_{h,\,max}$ [$\mu_{h,\,avg}$][a] [cm^2 V^{-1} s^{-1}]	V_{th} [V]	γ[b] [%]	$I_{on/off}$
PA4T[c]	N/A	0.012 (0.0093 ± 0.002)	–11	—[d]	10^4-10^5
	200	0.084 (0.082 ± 0.003)	–5	—[d]	10^4-10^5
PA4T-L	N/A	0.007 (0.0051 ± 0.001)	–4	87.2	10^3-10^4
	200	0.062 (0.046 ± 0.008)	–14	97.1	10^2-10^3
PA4T-C12-1	N/A	0.006 (0.0042 ± 0.001)	–15	83.6	10^3-10^4
	200	0.041 (0.023 ± 0.005)	–17	92.4	10^3-10^4
PA4T-C12-2	N/A	0.009 (0.0063 ± 0.002)	–18	79.1	10^4-10^5
	200	0.059 (0.040 ± 0.006)	–16	79.6	10^4-10^5
PA4T-Ra	N/A	0.23 (0.17 ± 0.032)	–3	86.8	10^3-10^4
	200	3.11 (2.39 ± 0.33)	–10	88.3	10^3-10^4

[a]Maximum mobility under optimized annealing conditions, average mobilities were calculated based on 10 independent devices and listed in parentheses. [b]Reliability factor γ calculated according to ref. [c]Reported previously; [d]Not available

Table S3. Summary of OFET device data for quinoid-donor polymers characterized by conventional spin-coating deposition method in recent 10 years.

Year	Materials	$\mu_{h,max}$ [cm^{2}v^{-1}s^{-1}]	Solvents	Device structure	References
2013	BPT-T	0.2	CB	TG/BC	*Chem. Commun.* 49, 2013, 4465.
2013	PPzDPDP-BT	0.066	CF	BG/BC	*Chem. Commun.* 49, 2013, 484.
2014	PTTD4T-DT	1.38	O-DCB	BG/TC	*J. Mater. Chem. C.* 2014, 2, 2307.

2016	PBTD4T	0.16	O-DCB	BG/TC	*J. Am. Chem. Soc.* 138, 2016, 7725.
2016	PBDTD4T	0.3	O-DCB	BG/TC	*J. Am. Chem. Soc.* 138, 2016, 7725.
2017	P-AQM3T-DT	0.54	CB	BG/TC	*J. Am. Chem. Soc.* 139, 2017, 8355.
2017	NDP-2T	0.67	CF	BG/BC	*Polym. Chem.* 2017,8, 3255-3260
2018	PQuT-T	3.6	O-DCB	TG/BC	*Adv. Mater.* 2018, 30, 1706557.
2018	PQuT-BT	2.77	O-DCB	TG/BC	*Adv. Mater.* 2018, 30, 1706557.
2019	PIQTT	0.13	CB	BG/TC	*Macromolecules.* 2019, 52, 4749.
2022	PAQM2T-TVT	0.0385	O-DCB	BG/BC	*Mater. Adv.* 2022, 3, 6853–6861
2023	PQ-2	0.003	CB	BG/TC	Mater. Adv. 2023,4, 1927-1934

Table S4. OFET performances of the second batch of PA4T-Ra polymer.

M_n[a] [kDa]	PDI	$\mu_\mathrm{h,\,max}$ [$\mu_\mathrm{h,\,avg}$][b] [$\mathrm{cm^2\,V^{-1}\,s^{-1}}$]	V_th [V]	γ[c] [%]	$I_\mathrm{on/off}$
22.3	2.7	2.98 (2.29 ± 0.31)	–2	86.5	10^3-10^4

[a] Molecular weight by high temperature SEC. [b] Maximum mobility under optimized annealing conditions, average mobilities were calculated based on 10 independent devices and listed in parentheses. [c] Reliability factor γ calculated according to ref.

Table S5. THF-processed OFET performance and reliability factors of the five polymers.

Polymer	$\mathrm{T_{annealing}}$ [°C]	$\mu_\mathrm{h,\,max}$ [$\mu_\mathrm{h,\,avg}$][a] [$\mathrm{cm^2\,V^{-1}\,s^{-1}}$]	V_th [V]	γ [%]	$I_\mathrm{on/off}$
PA4T	200	0.019 (0.013 ± 0.004)	–20	80.2	10^3-10^4
PA4T-L	200	0.017 (0.011 ± 0.002)	–16	83.1	10^3-10^4
PA4T-C12-1	200	0.014 (0.009 ± 0.001)	–24	73.6	10^2-10^3
PA4T-C12-2	200	0.022 (0.014 ± 0.004)	–27	71.5	10^4-10^5
PA4T-Ra	200	0.83 (0.56 ± 0.13)	–10	86.7	10^2-10^3

[a] Maximum mobility under optimized annealing conditions, average mobilities were calculated based on 10 independent devices and listed in parentheses.

8. References

1. Gaussian 09, Revision E.01, Frisch, M. J., Trucks, G. W., Schlegel, H. B., Scuseria, G. E., Robb, M. A., Cheeseman, J. R., Scalmani, G., Barone, V., Mennucci, B., Petersson, G. A., Nakatsuji, H., Caricato, M., Li, X., Hratchian, H. P., Izmaylov, A. F., Bloino, J., Zheng, G., Sonnenberg, J. L., Hada, M., Ehara, M., Toyota, K., Fukuda, R., Hasegawa, J., Ishida, M., Nakajima, T., Honda, Y., Kitao, O., Nakai, H., Vreven, T., Montgomery, J. A., Jr., Peralta, J. E., Ogliaro, F., Bearpark, M., Heyd, J. J., Brothers, E., Kudin, K. N., Staroverov, V. N., Kobayashi, R., Normand, J., Raghavachari, K., Rendell, A., Burant, J. C., Iyengar, S. S., Tomasi, J., Cossi, M., Rega, N., Millam, J. M., Klene, M., Knox, J. E., Cross, J. B., Bakken, V., Adamo, C., Jaramillo, J., Gomperts, R., Stratmann, R. E., Yazyev, O., Austin, A. J., Cammi, R., Pomelli, C., Ochterski, J. W., Martin, R. L., Morokuma, K., Zakrzewski, V. G., Voth, G. A., Salvador, P., Dannenberg, J. J., Dapprich, S., Daniels, A. D., Farkas, Ö., Foresman, J. B., Ortiz, J. V., Cioslowski, J., Fox, D. J. Gaussian, Inc., Wallingford CT, **2009**.
2. A. D. Becke, *J. Chem. Phys.*, 1993, **98**, 5648-5652.
3. W. J. Hehre, R. Ditchfield and J. A. Pople, *J. Chem. Phys.*, 2003, **56**, 2257-2261.
4. P. C. Hariharan and J. A. Pople, *Theor. Chim. Acta*, 1973, **28**, 213-222.
5. S. Grimme, S. Ehrlich and L. Goerigk, *J. Comput. Chem.*, 2011, **32**, 1456-1465.
6. G. Kresse and J. Furthmüller, *Phys. Rev. B*, 1996, **54**, 11169-11186.
7. P. E. Blochl, *Phys. Rev. B*, 1994, **50**, 17953-17979.
8. B. B. Hsu, C. M. Cheng, C. Luo, S. N. Patel, C. Zhong, H. Sun, J. Sherman, B. H. Lee, L. Ying, M. Wang, G. Bazan, M. Chabinyc, J. L. Bredas and A. Heeger, *Adv. Mater.*, 2015, **27**, 7759-7765.
9. L. Ye, W. Li, X. Guo, M. Zhang and H. Ade, *Chem. Mater.*, 2019, **31**, 6568-6577.
10. Z. Wang, Y. Shi, Y. Deng, Y. Han and Y. Geng, *Adv. Funct. Mater.*, 2021, **31**.
11. Z. F. Yao, Z. Y. Wang, H. T. Wu, Y. Lu, Q. Y. Li, L. Zou, J. Y. Wang and J. Pei, *Angew. Chem. Int. Ed.*, 2020, **59**, 17467-17471.